other evidence.[5,10] However, the chemical composition (e.g. both acidic and basic diol substrate binding sites?) and the structure of the active site, and thus further mechanistic insights, will require an X-ray diffraction structural analysis for at least one of the B_{12}-dependent enzymes.[25] Such crystallographic results will also test the one assumption on which this work, and the interpretations herein, are based, the assumption that the enzyme chemistry differs in degree, *but not in kind*, vs a *close* solution mimic.[26]

(25) The crystallization and preliminary diffraction data of an inactive form of methylmalonyl-CoA mutase has been published recently: Marsh, N.; Leadlay, P. F.; Evans, P. R. *J. Mol. Biol.* **1988**, *200*, 421.
(26) Holm, R. H. *Acc. Chem. Res.* **1977**, *10*, 427. See the related remark on p 427 and ref 2 therein.

Acknowledgment. We wish to thank the NIH for their financial support (Grant DK-26214).

Supplementary Material Available: Figure A, showing a ^1H NMR spectrum of **5** (1 page). Ordering information is given on any current masthead page.

Department of Chemistry
University of Oregon
Eugene, Oregon 97403

Yun Wang
Richard G. Finke*

Received September 29, 1988

Articles

Contribution from the Department of Chemistry,
Purdue University, West Lafayette, Indiana 47907

Non-Metal Redox Kinetics: Hypochlorite and Hypochlorous Acid Reactions with Sulfite

Kimber D. Fogelman, Dennis M. Walker, and Dale W. Margerum*

Received July 6, 1988

Pulsed-accelerated-flow spectroscopy is used in the ultraviolet region to measure pseudo-first-order rate constants in the range 5000–107 000 s^{-1} for the reactions of excess SO_3^{2-} with HOCl and OCl^- in the presence of HCO_3^-/CO_3^{2-} buffer. The rate constant for the reaction of HOCl and SO_3^{2-} is so large (7.6×10^8 M^{-1} s^{-1}, 25.0° C, $\mu = 0.5$) that the rate of proton transfer from water or from HCO_3^- to OCl^- can limit the reaction velocity. A mechanism with Cl^+ transfer to sulfur is proposed via a reactive intermediate, $HOClSO_3^{2-}$, that decomposes by itself or with HCO_3^- assistance to form $ClSO_3^-$. The subsequent hydrolysis of $ClSO_3^-$ to give Cl^- and SO_4^{2-} is slow by comparison (270 s^{-1}). The contribution of the HOCl path is small only above 0.05 M OH^-, where the rate becomes base-independent due to the reaction between OCl^- and SO_3^{2-} (2.3×10^4 M^{-1} s^{-1}, 25.0 °C, $\mu = 0.5$). This reaction may proceed by oxygen atom transfer; the rate constant is a factor of 3.3×10^4 smaller than the Cl^+-transfer rate constant for HOCl and SO_3^{2-}.

Introduction

The oxidation of sulfite ion by hypochlorite is fast and has a simple stoichiometry (eq 1). A rate constant for this reaction

$$OCl^- + SO_3^{2-} \xrightarrow{k_1} Cl^- + SO_4^{2-} \quad (1)$$

was initially measured by Lister and Rosenblum[1] 25 years ago by use of a continuous-flow mixer mounted on a trolley that moved the observation tube through the light path of a spectrophotometer. The value they obtained for k_1 was 1.1×10^4 M^{-1} s^{-1} (30.0 °C, $\mu = 0.62$), which was independent of base concentration from 0.05 to 0.20 M NaOH. Although they discussed the reaction as an example of an oxygen atom transfer process, there is no direct evidence that it occurs by this path.

Halperin and Taube[2] measured ^{18}O exchange for the reactions of sulfite with chlorate and with chlorite and concluded that oxygen atom transfer occurred in both cases. They ruled out a mechanism that involved intermediates with S–Cl bonds for these reactions. However, their results with hypochlorous acid and sulfite showed no evidence of oxygen atom transfer from the oxidizing agent to sulfite. This reaction was carried out in 0.2 M HCl, and the experiment was regarded as inconclusive because of rapid oxygen exchange between HOCl and H_2O via the Cl_2 equilibrium. They suggested two possible modes of reaction: one by oxygen atom transfer (where eq 1 is the elementary reaction) and the other via formation of chlorosulfate followed by its rapid hydrolysis. They did not reach any conclusions about which mechanism was predominant. The high concentration of HCl used in their study complicated the chemistry because of the formation of HOCl, Cl_2, SO_3H^-, and SO_2.

In recent work Yiin and Margerum[3] showed by stopped-flow indicator experiments that chlorosulfate is indeed an intermediate in the reaction of hypochlorous acid with sulfite (eq 2 and 3). The rate constant (k_h) for the hydrolysis of $ClSO_3^-$ at 25.0 °C is 270 s^{-1}.

$$HOCl + SO_3^{2-} \rightarrow OH^- + ClSO_3^- \quad (2)$$

$$ClSO_3^- + H_2O \xrightarrow{k_h} SO_4^{2-} + Cl^- + 2H^+ \quad (3)$$

Srivastava et al.[4] used a flow thermal method to study the OCl^- and SO_3^{2-} reaction. They reported a k_1 value of 6.75×10^3 M^{-1} s^{-1} at 30 °C and did not control the ionic strength, which varied from 0.008 to 0.036. They stated that the reaction rate did not change over the pH range 9.4–11.5. This is contrary to our results, because we observe an enormous increase in rate below pH 12. It may be that their measuring device was not capable of following faster reactions or that they were observing the hydrolysis of $ClSO_3^-$ rather than its formation. Although their discussion[4] suggests that HOCl rather than OCl^- is the reactant, this disagrees with their own lack of a pH effect.

Walker[5] used stopped-flow spectroscopy to estimate a rate constant of 2.5×10^4 M^{-1} s^{-1} for the reaction of OCl^- and SO_3^{2-} at 25.0 °C, $\mu = 0.50$. He examined a wider range of OH^- concentrations (0.25–0.005 M NaOH) than had been tested by Lister[1] and observed a large increase in the rate below 0.03 M [OH^-]. Below pH 11.5, the reactions are too fast to measure by conventional stopped-flow instruments. However, the pulsed-accelerated-flow (PAF) method[6,7] has been used to measure first-order rate constants as large as 124 000 s^{-1}. If a sufficiently large absorbance change is used, even larger first-order constants (180 000 s^{-1}) can be measured.[8] Until recently, PAF instru-

(1) Lister, M. W.; Rosenblum, P. *Can. J. Chem.* **1963**, *41*, 3013–3020.
(2) Halperin, J.; Taube, H. *J. Am. Chem. Soc.* **1952**, *74*, 375–380.
(3) Yiin, B. S.; Margerum, D. W. *Inorg. Chem.* **1988**, *27*, 1670–1672.
(4) Srivastava, R. D.; Nigam, P. C.; Goyal, S. K. *Ind. Eng. Chem. Fundam.* **1980**, *19*, 207–209.
(5) Walker, D. M. M.S. Thesis, Purdue University, 1981.
(6) Jacobs, S. A.; Nemeth, M. T.; Kramer, G. W.; Ridley, T. Y.; Margerum, D. W. *Anal. Chem.* **1984**, *56*, 1058–1065.
(7) Nemeth, M. T.; Fogelman, K. D.; Ridley, T. Y.; Margerum, D. W. *Anal. Chem.* **1987**, *59*, 283–291.

0020-1669/89/1328-0986$01.50/0

Table I. Protonation Constants for Reactants and Buffers[a]

species	log K_H	ref
OCl^-	7.50	*b*
SO_3^{2-}	6.60	*c*
CO_3^{2-}	9.70	*d*, *e*
OH^-	13.72 (pK_w)	*f*

[a] Conditions: 25.0 °C, μ = 0.50 ($NaClO_4$). [b] Reference 25. [c] Mesmer, R. E.; Baes, C. F. *J. Solution Chem.* **1974**, *3*, 307–321. [d] Odier, M.; Plichon, V. *Anal. Chim. Acta* **1971**, *55*, 209–220. [e] This work. [f] Sweeton, F. H.; Mesmer, R. E.; Baes, C. F. *J. Solution Chem.* **1974**, *3*, 191–214.

mentation was not available for use in the ultraviolet spectral region, but we now have a UV–PAF instrument[9] that can readily observe the loss of OCl^- at 292 nm (ϵ_{292} = 350 M^{-1} cm^{-1}) with rate constants in the range 5000–120 000 s^{-1}. In the present work, we use this instrument, together with stopped-flow results, to study the effect of a wide range of hydroxide and buffer concentrations on the kinetics of the reactions between hypochlorite and sulfite. Relatively little is known about the mechanisms of fast non-metal redox reactions of this type, despite their fundamental importance.

Experimental Section

Reagents. Stock solutions of sodium hydroxide, sodium chloride, sodium carbonate, and sodium hydrogen carbonate were prepared by dilution of the analytical grade reagents into doubly deionized water. The concentration of the NaOH stock solution, protected from CO_2 contamination, was determined by titration against potassium hydrogen phthalate with phenolphthalein indicator. A stock solution of sodium perchlorate was prepared from recrystallized $NaClO_4$ and was standardized gravimetrically.

Reaction media, consisting of NaOH or mixtures of Na_2CO_3 and $NaHCO_3$, were adjusted to a total ionic strength of 0.50 with $NaClO_4$ or NaCl stock solutions. The media were vigorously purged with argon to remove dissolved oxygen. Pulsed-accelerated-flow media were degassed and blanketed with argon. Solutions of sodium hypochlorite (Mallinckrodt analytical reagent grade) were prepared by direct dilution into the appropriate medium. Stock solutions of sodium sulfite were prepared by dissolving the anhydrous solid into an argon-protected medium. Single dilutions from stock were made to prepare the reaction solutions, and the reaction was studied within a few minutes of this preparation to prevent loss of the excess reagent due to reaction with oxygen. Table I gives values of the protonation constants (K_H) for the reactants at 25.0 °C and μ = 0.50.

Measurements of $-\log [H^+]$ were made by means of pH electrodes calibrated by a strong acid ($HClO_4$) versus strong base (NaOH) titration at a constant ionic strength (μ = 0.50 $NaClO_4$). Data of both pH and absolute voltage were collected with an Orion Model 701A research pH meter for each addition of base. Voltage readings were analyzed by the method of Gran[10] to determine actual concentrations of H^+ at each titration point. A linear least-squares fit gave the relationship $-\log [H^+] = 0.9698\ (pH) + 0.30$.

Stopped-Flow Measurements. The kinetics of the reactions of hypochlorite with sulfite in sodium hydroxide medium (25.0 °C, μ = 0.50 $NaClO_4$ or NaCl) were followed by use of a Durrum stopped-flow spectrophotometer interfaced to a Hewlett-Packard Model 2100S computer. Time-dependent absorbance changes (A_t) that correspond to loss of OCl^- were measured at 292 nm (ϵ = 350 M^{-1} cm^{-1}) for at least 4 half-lives of each decay. Pseudo-first-order conditions were maintained with a 10-fold or greater excess of sulfite concentration. Linear and multiple-linear regression analyses of the data provided values for the initial absorbance (A_0), the final absorbance (A_∞) and the pseudo-first-order rate constant (k'_{obsd}) as defined by eq 4. When k'_{obsd} values are

$$A_t = (A_0 - A_\infty)e^{-k'_{obsd}t} + A_\infty \quad (4)$$

large, they are corrected for effects of mixing[11] by means of the relationship in eq 5. For our stopped-flow instrument, k_{mix} has been established to be 1.7×10^3 s^{-1}. Small corrections (2%) occur at rate constants as low as 40 s^{-1}, but corrections become necessary above 100 s^{-1}, where the systematic error significantly exceeds the random uncertainty of a single determination. The values of k_{obsd} reported are the average of at least four individual determinations. For rate constants greater than 150 s^{-1}, ensembles of three absorbance decays were averaged prior to analysis to improve signal-to-noise performance. Excellent agreement with the first-order kinetic model confirms the dependence of the reaction on $[OCl^-]$ described by eq 6.

$$k_{obsd} = k'_{obsd}/(1 - k'_{obsd}/k_{mix}) \quad (5)$$

$$-\frac{d[OCl^-]}{dt} = k_{obsd}[OCl^-] \quad (6)$$

Table II. PAF-IV Features[a]

wavelength range: 200–850 nm
double monochromator: low stray light (<0.04%)
active low-pass filtering
twin-path observation-flow cell: 10-jet radial mixer, 1.0-cm flow path, 2.0-cm observation path
reactant volume per push: 5–6 mL
velocity ramp (along observation path): 3.0–12.6 m/s
programmable velocity profiles
PC-based data acquisition system (250 points at 10^{-3} s/point)
range of first-order rate constants: 200–200 000 s^{-1}

[a] References 6 and 7 give design details of pulsed-accelerated-flow models II and III. Reference 9 gives the modifications used for PAF-IV.

Pulsed-Accelerated-Flow (PAF) Measurements. The PAF Model IV instrument used in this study has evolved from our first pulsed-flow instrument[12] and our earlier pulsed-accelerated-flow models, PAF-II[6] and PAF-III (with a twin-path observation cell).[7] Design changes in PAF-IV compared with earlier models include a double-grating monochromator, which allows both UV and visible observation capabilities and minimizes stray light. A commercially available microprocessor-based positioning system is used for accurate control of accelerated pushes by a vertically mounted syringe ram. The PAF-IV instrument also has significantly improved signal-to-noise (S/N) performance compared to PAF-III. Details of the construction and computer interfacing of PAF-IV will be provided elsewhere.[9] A summary of instrumental features is listed in Table II.

As in the stopped-flow study, SO_3^{2-} is held in at least 10-fold excess concentration over OCl^-. Velocity-dependent absorbance changes (A_v) at 292 nm correspond to the disappearance of OCl^- as it reacts with SO_3^{2-} within the twin-path mixing/observation cell of PAF-IV. Unlike the stopped-flow method, however, the 2.0-cm observation tube of the twin-path cell includes the initial mixing region, so that absorbance changes based on the entire reaction profile are observed without the dead-time limitations inherent in stopped-flow methods. Analysis of rate constants in this study used plots of M_{exptl} vs the flow velocity (v) in the observation tube. When the k_{obsd} value is large (>5000 s^{-1}), there is a linear relationship between M_{exptl} and V (eq 7) for the twin-path observation cell,

$$M_{exptl} = \frac{A_v - A_\infty}{A_0 - A_\infty} = \frac{100}{k_m} + \frac{100v}{k_{obsd}} \quad (7)$$

where each half of the full observation path is treated as an independent 0.01-m path length.[7] In eq 7, A_0 is the initial absorbance of the reactants, A_∞ is the final absorbance of the products, A_v is the instantaneous absorbance at each velocity sampled, k_m is a mixing proportionality constant, and k_{obsd} is the reaction rate constant.

The PAF method is based on previous continuous-flow methods with integrating observation.[13,14] Its unique aspect is that measurements are taken as the flow of the reaction mixture is accelerated within the observation tube. The fact that the degree of mixing increases with velocity permits the resolution of the chemical reaction from the physical mixing rate.[6,7] The PAF method shares the advantage of other continuous-flow techniques in that reactants are continuously refreshed during the observation so that the requirement for extremely rapid data sampling for fast reactions is removed and higher precision can be obtained. However, the PAF method does not require large volumes of reagents because a single accelerated push allows a range of velocities (3.0–12.6 m s^{-1}) to be sampled but uses only 5–6 mL of each reagent. As outlined earlier,[6,7] the key feature of this method is that the variable velocity profile permits the chemical rate process to be resolved from the physical mixing processes without the necessity of external calibration curves. Three to five

(8) Nagy, J. C.; Dickson, P. N.; Margerum, D. W. To be submitted for publication.
(9) Bowers, C. P.; Fogelman, K. D.; Nagy, J. C.; Ridley, T. Y.; Wang, Y. L.; Margerum, D. W. To be submitted for publication.
(10) Rossotti, F. J. C.; Rossotti, H. *J. Chem. Educ.* **1965**, *42*, 375–378.
(11) Dickson, P. N.; Margerum, D. W. *Anal. Chem.* **1986**, *58*, 3153–3158.
(12) Owens, G. D.; Taylor, R. W.; Ridley, T. Y.; Margerum, D. W. *Anal. Chem.* **1980**, *52*, 130–138.
(13) Gerischer, H.; Heim, W. *Z. Phys. Chem. (Munich)* **1965**, *46*, 345–352.
(14) Gerischer, H.; Heim, W. *Ber. Bunsen-Ges. Phys. Chem.* **1967**, *171*, 1040–1046.

Table III. Pseudo-First-Order Rate Constants from Stopped-Flow Measurements of Excess SO_3^{2-} with OCl^- in OH^- Medium[a]

$[OH^-]$, M	$10^4[OCl^-]$, M	k_{obsd},[b] s^{-1}	$[OH^-]$, M	$10^4[OCl^-]$, M	k_{obsd},[b] s^{-1}
0.2372	0.4	28 (2)	0.0158	1.1	76 (9)
0.1898	0.4	35 (2)	0.0095	1.1	102 (14)
0.1160	0.4	34 (2)	0.0048	1.1	185 (28)
0.1423	0.4	36 (2)	0.2000[c]	1.0	24.2 (0.4)
0.1186	0.4	35 (2)	0.1000[c]	1.0	26.7 (0.5)
0.0955	1.1	24 (2)	0.0200[c]	1.0	39 (1)
0.0477	1.1	36 (2)	0.0020[c]	1.0	254 (45)
0.0191	1.1	50 (2)			

[a] Conditions: 25.0 °C, μ = 0.50 ($NaClO_4$ + NaOH), $[SO_3^{2-}]_T$ = 1.00 × 10^{-3} M, λ_{obsd} = 292 nm. [b] Values in parentheses denote 1 standard deviation. [c] μ = 0.50 (NaCl + NaOH).

PAF runs were measured for each set of conditions, and average k_{obsd} values are reported with their standard deviations.

Resolution of Individual Rate Constants. After the k_{obsd} values were measured for each set of reaction conditions, a method was needed to iteratively estimate individual rate constants for each step of a proposed mechanism and compare these estimates to the observed data. The program Lotus 1-2-3 (version 2.10) was used for this purpose. With this program, it was possible to recalculate predicted reaction rate constants quickly for any change in one of the individual rate constants. Also, it was very easy to graphically demonstrate the fit of each set of estimates to all variation studies. Further, as it became apparent that a more complex model was necessary to explain all the data, the graphical displays were adjusted to demonstrate the differences in predicted rate constants for each new model proposed. By this means it was possible to select the most appropriate mechanism and optimize the fit to all the observed data. It should be noted that this method was considerably more successful than optimizing an individual variation study by means of simplex[15] fitting because of the inconsistencies these fits produced in the other variation studies.

The program GEAR[16,17] was used to construct a profile of $[OCl^-]$ vs time for our final set of rate constants. This program takes in up to 60 individual reaction steps and the corresponding rate constants as well as initial concentration values for each chemical species. The advantage of using GEAR in this study is that estimates for all possible reaction steps may be included without having to solve the integrated expression. Thus, very complicated mechanisms can be evaluated without the restrictions of assuming steady-state or irreversible reaction conditions.

The output data of $[OCl^-]$ vs time were analyzed by an off-line, first-order analysis program. The resulting k_{obsd} values were in good agreement with the k_{obsd} values calculated by the PAF analysis software. In addition, the GEAR-generated data were examined for goodness of fit to the first-order exponential model. Excellent agreement was found, which indicates that the first-order model is appropriate for the PAF reaction conditions studied.

Results and Discussion

Reactions in NaOH Solutions. Table III summarizes the reagent concentrations and the resolved pseudo-first-order rate constants obtained from stopped-flow experiments, where $[SO_3^{2-}]$ was held in at least 10-fold excess and the disappearance of OCl^- was monitored at 292 nm. Individual runs of ln $(A_t - A_\infty)$ vs time gave excellent linear plots to establish the first-order dependence in $[OCl^-]$. The plot of k_{obsd} values against excess SO_3^{2-} concentration in 0.0955 M NaOH (Figure 1) is linear with a negligible intercept and demonstrates a first-order dependence in sulfite concentration.

Our data in Table III and Figure 2 show a dramatic increase in k_{obsd} as the concentration of OH^- is reduced below 0.050 M. This dependence indicates two reaction paths, where hydroxide ion inhibits one path in accord with eq 8. A weighted least-squares

$$k_{obsd} = \left(k_1 + \frac{k_2}{[OH^-]}\right)[SO_3^{2-}] \qquad (8)$$

analysis that takes into account the precision of all the k_{obsd} values

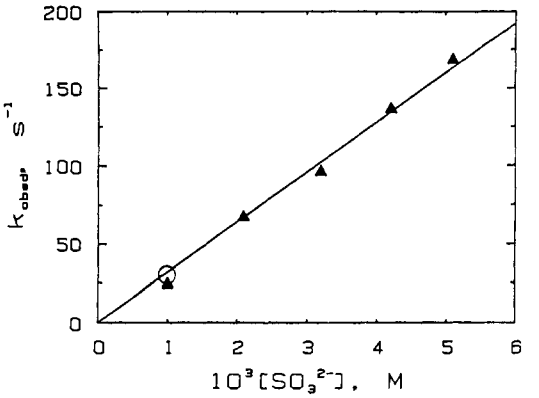

Figure 1. Pseudo-first-order rate constants (25.0 °C, μ = 0.5 ($NaClO_4$)) from stopped-flow measurements of OCl^- with excess SO_3^{2-} in 0.0955 M NaOH (▲), and from the fit of data in Figure 2 to this NaOH concentration (○).

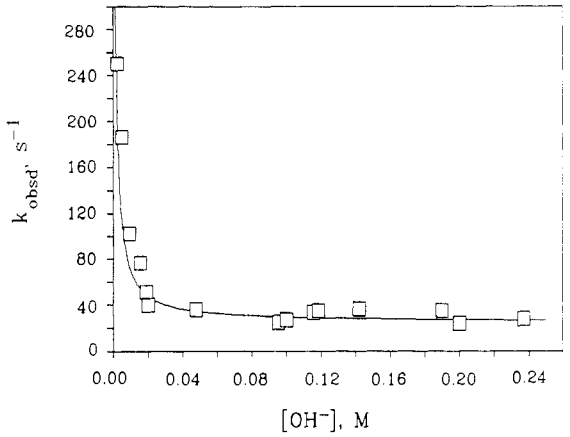

Figure 2. Effect of NaOH concentration on the pseudo-first-order rate constant for the reaction of OCl^- with excess SO_3^{2-} (1.0 × 10^{-3} M). The solid line is calculated from eq 8.

in Table III (in both $NaClO_4$ and in NaCl media) gives k_1 = (2.3 ± 0.2) × 10^4 M^{-1} s^{-1} and a value of 450 ± 30 s^{-1} for k_2. The line in Figure 2 is calculated from these values. Hence, our results agree with those of Lister and Rosenblum[1] in regard to reaction order, and we agree that the observed rate constant remains largely independent of hydroxide ion concentration above 0.05 M NaOH. However, our value for k_1 at 25.0 °C and 0.50 μ is twice as large as their value of 1.1 × 10^4 M^{-1} s^{-1} at 30.0 °C and μ = 0.62 (NaCl). They determined the activation energy (7.5 kcal mol^{-1}) and showed that there was little ionic strength dependence in this region. We tested to be sure that Cl^- did not have a special effect compared to ClO_4^- and found no appreciable difference for the rate constants in NaCl vs $NaClO_4$ media (Table III). Hence, the reason for this discrepancy is not clear. The stopped-flow mixing and measuring system that we used is much better suited to study fast reactions than was Lister's system, where second-order conditions were needed. The sensitivity of their instrument was much poorer, and mixing limitations also may have contributed to give smaller rate constants.

The inverse hydroxide ion dependence indicates that the rate increases either by the reaction of HOCl with SO_3^{2-} or by the reaction of OCl^- with SO_3H^-. The mechanism with HOCl (pK_a = 7.5) treated as a steady-state species is given in eq 9 and 10 and the overall rate expression is given by eq 11. Values for

$$OCl^- + H_2O \underset{k_{-3}}{\overset{k_3}{\rightleftharpoons}} HOCl + OH^- \qquad (9)$$

$$HOCl + SO_3^{2-} \xrightarrow{k_4} \text{products} \qquad (10)$$

$$\frac{-d[OCl^-]}{dt} = \left(k_1 + \frac{k_3k_4}{k_{-3}[OH^-] + k_4[SO_3^{2-}]}\right)[OCl^-][SO_3^{2-}] \qquad (11)$$

(15) Caceci, M. S.; Catheris, W. P. *Byte* **1984**, *9*, 340–362.
(16) Beukelman, T. E.; Chesick, J.; McKinney, R. J.; Weigert, F. J. "GEAR"; E. I. du Pont de Nemours and Co., Wilmington, DE.
(17) GEAR is a modification of the HAVCHM program: Stabler, R. N.; Chesick, J. *Int. J. Chem. Kinet.* **1978**, *10*, 461–469.

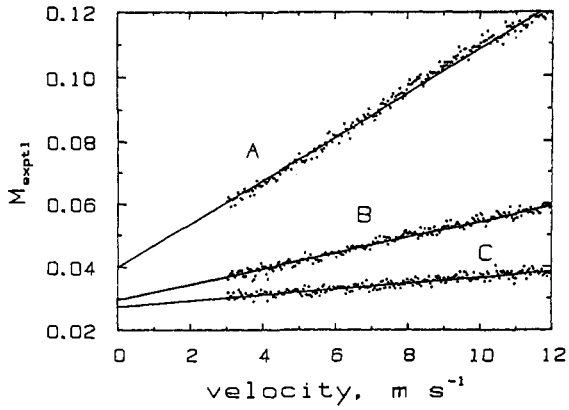

Figure 3. PAF-IV plots of eq 7 for OCl^- and SO_3^{2-} (10^{-2} M) in 0.1 M HCO_3^-/CO_3^{2-} buffer: (A) k_{obsd} = 13 600 s^{-1} (−log [H^+] = 10.30); (B) k_{obsd} = 39 100 s^{-1} (−log [H^+] = 9.88); (C) k_{obsd} = 107 000 s^{-1} (−log [H^+] = 9.53).

proton-transfer rate constants for oxygen acids with OH^- (such as k_{-3}) are typically between 10^9 and 10^{10} M^{-1} s^{-1}.[18] When [OH^-] > [SO_3^{2-}], the value of k_{-3}[OH^-] should be much greater than k_4[SO_3^{2-}] so that $k_2 = k_3k_4/k_{-3}$. The ratio of k_3/k_{-3} can be evaluated from $K_w/K_a = 6.0 \times 10^{-7}$ M where pK_w = 13.72 at 25.0 °C, μ = 0.5. This gives a k_4 value of $(7.6 \pm 0.4) \times 10^8$ M^{-1} s^{-1}. This value is consistent with the assumption that k_{-3}[OH^-] ≫ k_4[SO_3^{2-}] for the conditions in Table III. Although the k_4 value is large, it is an order of magnitude smaller than the diffusion-limited rate constant of 7×10^9 M^{-1} s^{-1} that is expected in water at 25 °C when one reactant is uncharged.[19]

An alternate mechanism is considered in eq 12 and 13, where SO_3H^- increases the reaction rate. Since the OCl^- concentration is much less than the SO_3^{2-} concentration in our experiments, we

$$SO_3^{2-} + H_2O \underset{k_{-a}}{\overset{k_a}{\rightleftharpoons}} SO_3H^- + OH^- \qquad (12)$$

$$SO_3H^- + OCl^- \xrightarrow{k_b} \text{products} \qquad (13)$$

could expect k_{-a}[OH^-] ≫ k_b[OCl^-], and therefore, $k_2 = (k_a/k_{-a})k_b$. The protonation constant for SO_3^{2-} is $10^{6.6}$ M^{-1}, so that $k_a/k_{-a} = 7.6 \times 10^{-8}$ and $k_b = 5.9 \times 10^9$ M^{-1} s^{-1}. The reactants are now both negatively charged, and for a center-to-center distance of 2.4 Å in the transition state and μ = 0.5, we estimate a maximum diffusion-controlled rate constant of 3×10^9 M^{-1} s^{-1}. Since the k_b value is a factor of 2 larger than this diffusion limitation, the mechanism in eq 12 and 13 cannot be a major contributor to the reaction rate. Furthermore, there are two protonated forms of hydrogen sulfite: one with the proton on the oxygen (SO_3H^-) and one with the proton on the sulfur (HSO_3^-).[20] The ratio of [SO_3H^-]/[HSO_3^-] is reported to be 4.9.[21] The HSO_3^- form is 2 orders of magnitude slower to transfer its proton.[22] With a proton on the sulfur atom, HSO_3^- would not be expected to be reactive with OCl^-. This increases the calculated k_b value for the SO_3H^- form to 7.1×10^9 M^{-1} s^{-1}, which is now a factor of 2.4 greater than the diffusion-controlled rate constant. Hence, no more than 30% of the overall rate could be carried by the SO_3H^- reaction with OCl^-.

Effect of Carbonate Buffer at High pH. As the hydroxide ion concentration is reduced below 0.002 M, the rate of the hypochlorite and sulfite reaction becomes too fast to measure by the stopped-flow method. However, the reactions are readily observed by the pulsed-accelerated-flow method at 292 nm with the PAF-IV instrument. Tests with several buffers showed that the rates are very sensitive to buffer concentrations as well as to the pH of the reaction mixture. A carbonate buffer system was selected in order to keep the pH constant during individual reactions and to investigate the effect of buffer concentration on the rate. Table IV summarizes the k_{obsd} values for each set of conditions used. Plots of M_{expt} against velocity in Figure 3 show three experimental conditions where the resolved k_{obsd} values are $(13.6 \pm 0.1) \times 10^3$ s^{-1}, $(39.4 \pm 0.9) \times 10^3$ s^{-1}, and $(107 \pm 2) \times 10^3$ s^{-1}. The signal-to-noise ratio and the reproducibility are excellent.

Figure 4 shows that when 0.200 M carbonate buffer is used at −log [H^+] values of 10.17–10.19, the observed first-order rate constants appear to be directly proportional to the SO_3^{2-} concentration. (To a first approximation a linear dependence of k_{obsd} with [SO_3^{2-}] exists, but the results in Table IV where [H^+] and [CO_3^{2-}]$_T$ are varied indicate a more complex dependence in [SO_3^{2-}]. It will be shown that there is a slight deviation from linearity that is hidden by small variations in the adjusted p[H^+] values.) Figure 5 shows the dependence of k_{obsd} as the carbonate buffer concentration is increased from 0.01 to 0.20 M at −log [H^+] = 10.26–10.31 with a sulfite concentration of 1.0×10^{-2} M. (The data do not give a smooth curve because of small variations in point-to-point p[H^+] values. The basis of the solid and dashed lines will be explained later.) If k_{-3} is 3×10^9 M^{-1} s^{-1}, then k_3 must be 1.8×10^3 s^{-1} in order to give the correct equilibrium constant for eq 9. Hence, in the absence of carbonate the k_{obsd} value (calculated from eq 11 for 10^{-2} M [SO_3^{2-}] and −log [H^+]

Table IV. Pseudo-First-Order Rate Constants from Pulsed-Accelerated-Flow Measurements in Carbonate-Buffered Medium for the Reaction of SO_3^{2-} with OCl^- and HOCl[a]

10^3[SO_3^{2-}]$_T$, M	[CO_3^{2-}]$_T$, M	−log [H^+]	$10^{-3}k_{obsd}$, s^{-1}
10.0	0.010	10.30	5.6 (0.1)
10.0	0.020	10.29	8.32 (0.04)
10.0	0.045	10.31	11.0 (0.1)
10.0	0.070	10.27	13.6 (0.1)
10.0	0.100	10.27	14.6 (0.1)
10.0	0.140	10.29	16.2 (0.1)
10.0	0.170	10.29	17.2 (0.1)
10.0	0.200	10.26	19.8 (0.2)
10.0	0.100	10.30	13.6 (0.1)
10.0	0.100	10.08	24.0 (0.5)
10.0	0.100	9.88	39.4 (0.9)
10.0	0.100	9.71	68 (1)
10.0	0.100	9.53	107 (2)
2.00[b]	0.200	10.19	4.83 (0.03)
6.03[b]	0.200	10.17	15.4 (0.2)
8.00[b]	0.200	10.18	20.6 (0.6)
10.0[b]	0.200	10.18	26.0 (0.8)

[a] Conditions: 25.0 °C, μ = 0.50, [OCl^-]$_T$ = 1.0×10^{-3} M, λ_{obsd} = 292 nm; k_{obsd} values are averaged for three to five runs, and values in parentheses denote 1 standard deviation. [b] [OCl^-]$_T$ = 0.20×10^{-3} M.

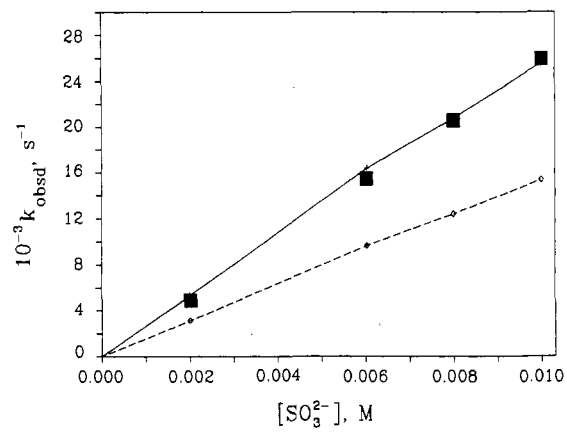

Figure 4. Pseudo-first-order rate constants for the reaction of excess SO_3^{2-} with OCl^-: PAF-IV; 292 nm; 0.20 M [CO_3^{2-}]$_T$; −log [H^+] = 10.18 ± 0.01; 25.0 °C; μ = 0.5. The solid line is a point-to-point calculation from eq 23 and the rate constants in Table V. The dashed line is calculated from the same constants with the k_6[HCO_3^-] path omitted.

(18) Eigen, M. *Angew. Chem. Int. Ed. Engl.* **1964**, *3*, 1–72.
(19) Caldin, E. F. *Fast Reactions in Solution*; Wiley: New York, 1964; p 12.
(20) Golding, R. M. *J. Am. Chem. Soc.* **1960**, 3711–3715.
(21) Horner, D. A.; Connick, R. E. *Inorg. Chem.* **1986**, *25*, 2414–2417.
(22) Horner, D. A. Ph.D. Thesis, University of California at Berkeley, 1984.

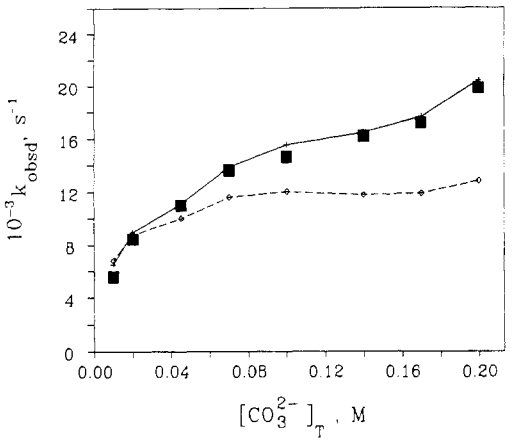

Figure 5. Pseudo-first-order rate constants for the reaction of OCl^- with excess SO_3^{2-} (10^{-2} M) as a function of $[CO_3^{2-}]_T$ at -log $[H^+]$ = 10.29 ± 0.02. The solid line is a point-to-point calculation from eq 23 and the rate constants in Table V. (Small variations in $[H^+]$ from point to point cause the staggered appearance of this line.) The dashed line is calculated from the same constants with the $k_6[HCO_3^-]$ path omitted.

= 10.3) cannot exceed 2000 s^{-1}. In the presence of carbonate an additional proton transfer path is available (eq 14) that leads to

$$OCl^- + HCO_3^- \underset{k_{-3'}}{\overset{k_{3'}}{\rightleftharpoons}} HOCl + CO_3^{2-} \qquad (14)$$

much larger k_{obsd} values as seen in Figure 5. A steady-state approximately (in regard to [HOCl]) gives the rate expression in eq 15.

$$\text{rate} = k_1[OCl^-][SO_3^{2-}] + \frac{k_4(k_3 + k_{3'}[HCO_3^-])[OCl^-][SO_3^{2-}]}{k_{-3}[OH^-] + k_{-3'}[CO_3^{2-}] + k_4[SO_3^{2-}]} \qquad (15)$$

The results in Figure 5 show that proton-transfer steps limit the reaction. This limitation would not occur if the reaction proceeded through OCl^- and SO_3H^-. To show that this is the case, consider the reactions in eq 12, 13, and 16 where SO_3H^- is the

$$SO_3^{2-} + HCO_3^- \underset{k_{-a'}}{\overset{k_{a'}}{\rightleftharpoons}} SO_3H^- + CO_3^{2-} \qquad (16)$$

reaction intermediate. A steady-state treatment in terms of SO_3H^- leads to eq 17. We have shown that k_b must be less than 3 ×

$$\text{rate} = k_1[OCl^-][SO_3^{2-}] + \frac{k_b(k_a + k_{a'}[HCO_3^-])[OCl^-][SO_3^{2-}]}{k_{-a}[OH^-] + k_{-a'}[CO_3^{2-}] + k_b[OCl^-]} \qquad (17)$$

10^9 M^{-1} s^{-1}. In our experiments hypochlorite is present as the limiting reagent, so its initial concentration is only one-tenth that of SO_3^{2-} and its final concentration approaches zero. Despite some charge repulsion, the value of $k_{-a'}$ will be at least as large as the value of $k_{-3'}$, because SO_3H^- is a stronger acid than HOCl. Hence, $k_{-a}[OH^-] + k_{-a'}[CO_3^{2-}]$ will be much larger than $k_b[OCl^-]$ under the conditions used. As a consequence, it can be shown that SO_3H^- will be present close to its equilibrium level at all carbonate concentrations and there should be no buffer dependence. The fact that an increase in the concentration of carbonate buffer causes a rate increase by a factor of 4 is additional evidence that it is the HOCl and SO_3^{2-} couple in eq 10, rather than the OCl^- and SO_3H^- couple in eq 13, that accelerates the reaction.

Effect of -log $[H^+]$ Variation with Carbonate Buffer. Figure 6 shows the first-order rate constants as values of -log $[H^+]$ are changed from 10.3 to 9.5 when $[SO_3^{2-}]$ is 10^{-2} M and $[CO_3^{2-}]_T$ is 0.10 M. The increase in the k_{obsd} values with decrease in pH is consistent with an increase in the rate of HOCl formation as a result of HCO_3^- reaction with OCl^-. However, below pH 10

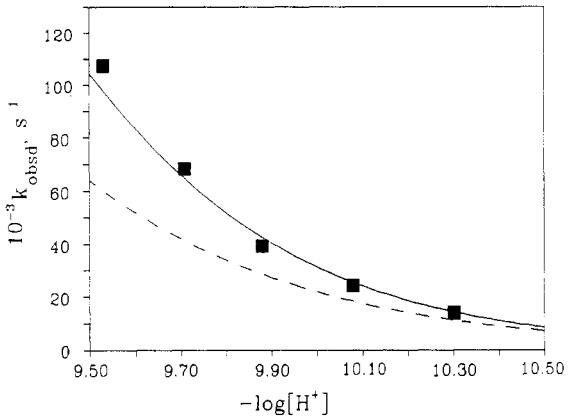

Figure 6. Pseudo-first-order rate constants as a function of -log $[H^+]$ for the reaction of OCl^- with excess SO_3^{2-} (10^{-2} M) and $[CO_3^{2-}]_T$ = 0.10 M. The solid line is a point-to-point calculation from eq 23 and the rate constants in Table V. The dashed line is calculated from the same constants with the $k_6[HCO_3^-]$ path omitted.

the k_{obsd} values increase much more than is predicted by eq 15. An additional HCO_3^- contribution to the rate of the reaction must occur to explain this behavior and to give a consistent fit for the data in Figures 4–6.

Proposed Mechanism. The reaction between HOCl and SO_3^{2-} can be written as a two-step process (eq 18 and 19) if $HOClSO_3^{2-}$

$$HOCl + SO_3^{2-} \underset{k_{-4'}}{\overset{k_{4'}}{\rightleftharpoons}} HOClSO_3^{2-} \qquad (18)$$

$$HOClSO_3^{2-} \xrightarrow{k_5} OH^- + ClSO_3^- \qquad (19)$$

is considered as a reaction intermediate rather than a transition state. This means that the k_4 rate constant from eq 10 is a composite of rate constants (eq 20). The value of $k_{4'}$ can be larger

$$k_4 = \frac{k_{4'}k_5}{k_{-4'} + k_5} \qquad (20)$$

than $k_{4'}$ and HCO_3^- assisted breakup of $HOClSO_3^{2-}$ (eq 21) will increase the rate of formation of products.

$$HOClSO_3^{2-} + HCO_3^- \xrightarrow{k_6} H_2O + CO_3^{2-} + ClSO_3^- \qquad (21)$$

In recent work evidence has been found[23] for a rapidly formed $HOClI^-$ intermediate in the reaction of HOCl and I^-. Since SO_3^{2-} is a stronger nucleophile than I^- it is reasonable to expect that $HOClSO_3^{2-}$ (structure I) can also form with two electron-pair

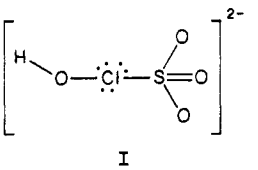

I

bonds and three lone pairs of electrons around chlorine. We propose that this intermediate reacts by O–Cl bond cleavage to give OH^- and $ClSO_3^-$ (eq 19) and by proton transfer from HCO_3^- to the oxygen adjacent to the chlorine to give H_2O + $ClSO_3^-$ (eq 21).

In high concentrations of HCO_3^-/CO_3^{2-} buffer the proton-transfer contribution from H_2O (eq 9) is negligible and the predicted k_{obsd} value can be obtained by a double steady-state derivation with HOCl and $HOClSO_3^{2-}$ as reactive intermediates. This gives eq 22, which can also be written as eq 23. The k_1 value

(23) Nagy, J. C.; Kumar, K.; Margerum, D. W. *Inorg. Chem.* **1988**, *27*, 2773–2780.

$$k_{obsd} = k_1[SO_3^{2-}] + (k_5 + k_6[HCO_3^-]) \times (k_{3'}k_{4'}[HCO_3^-][SO_3^{2-}])/(k_5 + k_6[HCO_3^-])(k_{-3'}[CO_3^{2-}] + k_{4'}[SO_3^{2-}]) + k_{-4'}k_{-3'}[CO_3^{2-}] \quad (22)$$

$$k_{obsd} - k_1[SO_3^{2-}] = k_{3'}[HCO_3^-](1 + k_6/k_5[HCO_3^-])[SO_3^{2-}]/\left(\frac{k_{-3'}}{k_{4'}}[CO_3^{2-}] + [SO_3^{2-}]\right)\left(1 + \frac{k_6}{k_5}[HCO_3^-]\right) + \frac{k_{-3'}k_{-4'}}{k_{4'}k_5}[CO_3^{2-}] \quad (23)$$

and the ratio $k_{4'}k_5/(k_{-4'} + k_5)$ are obtained from stopped-flow data. The ratio $k_{3'}/k_{-3'}$ ($=10^{-2.20}$) is known from the pK_a values of HCO_3^- (9.70) and HOCl (7.50). The minimum number of additional constants needed to fit eq 23 are $k_{3'}$, or $k_{-3'}$, k_6/k_5, and $k_{-3'}/k_{4'}$. The $k_{-4'}/k_5$ ratio is fixed by these parameters, the experimental k_4 value, and eq 20. The 17 data points in Table IV with variation of $[CO_3^{2-}]_T$, $[SO_3^{2-}]$, and $[H^+]$ provide severe constraints upon the choice of these constants. The solid curves plotted in Figures 4–6 correspond to values of $k_{-3'} = 1.0 \times 10^9$ M^{-1} s^{-1}, $k_{-3'}/k_{4'} = 0.20$, and $k_6/k_5 = 20$ M^{-1}. Each of these constants has a precision of approximately ±10% in order to obtain the best fit. The relative standard deviation of the residuals for all 17 PAF data points from the calculated values is ±5%. The solid lines plotted in Figure 5 are calculated from a Lotus 1-2-3 program on a point-to-point basis because of slight variations in −log $[H^+]$ values. A small increase in $[H^+]$ is partly responsible for the upward curvature at the highest $[CO_3^{2-}]_T$ value in this figure. The $k_{-3'}$ value of 1.0×10^9 M^{-1} s^{-1} is very reasonable for a proton-transfer reaction with a favorable $\Delta(pK_a)$ change (+2.3 units) and agrees well with similar rate constants measured by Eigen.[18] Table V gives a summary of all the rate constants resolved from the stopped-flow and PAF data. This includes an estimated value for $k_{-3} = 3 \times 10^9$ M^{-1} s^{-1} for the reaction of OH^- with HOCl. This value is chosen to be larger than $k_{-3'}$ (as expected for reactions of OH^- compared to other bases) to fit the stopped-flow data at the lowest hydroxide ion concentrations and to avoid interference with the fit of the lowest $[CO_3^{2-}]_T$ data.

Equation 23 has a $[SO_3^{2-}]$ term in the denominator as well as in the numerator, but the k_{obsd} values in Figure 4 appear to have a simple first-order dependence in $[SO_3^{2-}]$. Under the conditions used the contribution of $[SO_3^{2-}]$ to the denominator value is small. When $[SO_3^{2-}]$ equals 0.01 M, the denominator term causes k_{obsd} to be 92% of the directly proportional value. The point-to-point solid line in Figure 4 is calculated from eq 23, the data in Table IV, and the rate constants in Table V. The plot shows how sensitive the calculation is to a small variation of p$[H^+]$ (0.02 units), which effectively masks the slight deviation from first-order $[SO_3^{2-}]$ dependence. The calculated line shows excellent agreement with the experimental data. This is also the case for the calculated rate constants from eq 23 in Figures 5 and 6. The enormous increase in k_{obsd} values shown in Figure 6 as the p$[H^+]$ decreases to 9.5 requires a significant contribution from the k_6 path (eq 21). The p$[H^+]$ fluctuation of 0.05 units for the data in Figure 5 is a result of experimental difficulty in the preparation of exactly matched p$[H^+]$ when the $[CO_3^{2-}]_T$ is varied from 0.01 to 0.20 M. This small variation in p$[H^+]$ from point to point causes the staggered appearance of the experimental k_{obsd} values. Nevertheless, the calculated k_{obsd} values reflect the same behavior and agree very well with the experimental values.

The dashed curves in Figures 4–6 show the calculated rate constants based on eq 15, where the $k_6[HCO_3^-]$ path is neglected. It can be seen that, under these conditions, the additional path with HCO_3^--assisted breakup of $HOClSO_3^{2-}$ (eq 21) is quite important. In the proposed transition state (structure II) a proton is transferred to the HO group as the O–Cl bond is broken. High ionic strength (0.50) and the wide separation of charges in II help to make this path significant despite the build up of a −3 charge in the transition state. Similar mechanisms were found[24] for

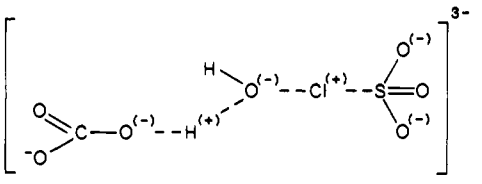

II

acid-assisted reactions between NH_2Cl and SO_3^{2-}.

Formation and Hydrolysis of $ClSO_3^-$. The formation and decay of $ClSO_3^-$ (eq 24, 25) are not directly observed in the stopped-flow and PAF measurements, because $ClSO_3^-$ has negligible absorbance

$$H_2O + OCl^- + SO_3^{2-} \rightarrow 2OH^- + ClSO_3^- \quad (24)$$

$$ClSO_3^- + 2OH^- \rightarrow Cl^- + SO_4^{2-} + H_2O \quad (25)$$

at 292 nm where the disappearance of OCl^- is followed. These reactions are a possible explanation of the discrepancy between our results and the results of Srivastava et al.,[4] where the rate of the OCl^- and SO_3^{2-} reaction appeared to have no pH dependence. We measured the rate of loss of OCl^-, while they[4] measured the heat of the reaction. It is likely that the formation of $ClSO_3^-$ (eq 24) will generate little heat, while the base hydrolysis of $ClSO_3^-$ (eq 25) will be very exothermic. Since they did not find a change in reaction rate between pH 9.4 and 11.5, it may be that OH^- does not accelerate the hydrolysis of $ClSO_3^-$ in this pH range.

Since $ClSO_3^-$ has negligible absorbance at 292 nm, the measurement is not affected by a change of the principle products from Cl^- and SO_4^{2-} under stopped-flow conditions to $ClSO_3^-$ under PAF conditions. The overall reaction (eq 1) has no pH change, but two OH^- ions are released for each OCl^- that is converted to $ClSO_3^-$. At the lowest hydroxide ion concentration (0.002 M) used in the stopped-flow study, the rate constant for the aqueous hydrolysis of $ClSO_3^-$ is only slightly larger than its formation constant. The rate of hydrolysis of $ClSO_3^-$ is constant from pH 3.5 to pH 9,[3] and may not increase at higher pH. Hence, it is possible for some $ClSO_3^-$ and OH^- to build up during the reaction. However, the initial concentration of OCl^- is only 1×10^{-4} M, so the increase of OH^- is too small to affect the k_{obsd} value within the experimental precision of this constant (18%).

Under PAF reaction conditions, the hydrolysis of $ClSO_3^-$ is negligible (unless it is catalyzed by OH^-) in the region of the mixing cell where the loss of OCl^- is observed. The initial OCl^- concentration is 1.0×10^{-3} M, so that at the lowest $[CO_3^{2-}]_T$ value of 0.010 M (initial −log $[H^+]$ = 10.3) the buffer capacity of HCO_3^-/CO_3^{2-} is exceeded and we estimate that −log $[H^+]$ approaches 10.5 during the PAF measurement. (After the experiment the value is 10.3 because $ClSO_3^-$ has hydrolyzed.) The increase in −log $[H^+]$ accounts for the deviation of this experimental point from the calculated value. As the amount of $[CO_3^{2-}]_T$ is increased for other data points, this discrepancy is removed.

GEAR **Analysis of the Proposed Mechanism Compared to the Steady-State Model.** Equation 23 is a steady-state approximation that omits proton-transfer contributions from H_2O (eq 9), from eq 16, and from eq 26, because these terms were estimated to be

$$SO_3H^- + OCl^- \rightleftharpoons SO_3^{2-} + HOCl \quad (26)$$

small or negligible at high concentrations of carbonate buffer. The GEAR program permits a test of the combined effect of all these rate constants together with those in eq 1, 3, 14, 18, 19, and 21, without recourse to steady-state approximations. The resultant output of the concentration of OCl^- against time gave excellent first-order plots that agreed with the rate constants obtained from the iterative fits of eq 23 to the data in Table IV. Thus there are no hidden contributions to the rate. It is interesting that for the 0.010 M $[CO_3^{2-}]_T$ condition (the lowest point in Figure 5), the GEAR program shows a small buildup and decay of OH^- and indicates that the decay of OCl^- is only approximately first order. Furthermore, the calculated k_{obsd} value from the GEAR program is in much better agreement with the experimental data than the value calculated from eq 23, which neglected the small change in $[OH^-]$.

(24) Yiin, B. S.; Walker, D. M.; Margerum, D. W. *Inorg. Chem.* **1987**, *26*, 3435–3441.

Table V. Summary of Rate Constants[a]

reactions	rate constants[b]
$OCl^- + SO_3^{2-} \rightarrow Cl^- + SO_4^{2-}$	$k_1 = (2.3 \pm 0.2) \times 10^4\ M^{-1}\ s^{-1}$
$OCl^- + H_2O \rightleftarrows HOCl + OH^-$	$k_3 = 1.8 \times 10^3\ s^{-1}$ $k_{-3} = 3.0 \times 10^9\ M^{-1}\ s^{-1}$
$OCl^- + HCO_3^- \rightleftarrows HOCl + CO_3^{2-}$	$k_{3'} = 6.3 \times 10^6\ M^{-1}\ s^{-1}$ $k_{-3'} = 1.0 \times 10^9\ M^{-1}\ s^{-1}$
$HOCl + SO_3^{2-} \rightarrow OH^- + ClSO_3^-$	$k_4 = k_4k_5/(k_{-4'} + k_5) = (7.6 \pm 0.4) \times 10^8\ M^{-1}\ s^{-1}$
$HOCl + SO_3^{2-} \rightleftarrows HOClSO_3^{2-}$	$k_{4'} = 5.0 \times 10^9\ M^{-1}\ s^{-1}$ $k_{-4'}/k_5 = 5.6$
$HOClSO_3^{2-} \xrightarrow{k_5} OH^- + ClSO_3^-$	
$HCO_3^- + HOClSO_3^{2-} \xrightarrow{k_6} H_2O + CO_3^{2-} + ClSO_3^-$	$k_6/k_5 = 20\ M^{-1}$
$ClSO_3^- + H_2O \xrightarrow{k_h} Cl^- + SO_4^{2-} + 2H^+$	$k_h = (2.7 \pm 0.2) \times 10^2\ s^{-1}$[c]

[a] Conditions: 25.0 °C, μ = 0.50. [b] A precision of ±10% is estimated unless otherwise specified. [c] Reference 3.

Table VI. Comparison of HOCl and NH_3Cl^+ Rate Constants with Nucleophiles[a]

reactants	k, $M^{-1}\ s^{-1}$	ref	n[b]
$HOCl + Br^-$	1.55×10^3	23	3.89
$HOCl + I^-$	1.4×10^8	22	5.04
$HOCl + SO_3^{2-}$	7.6×10^8	*c*	5.1
$NH_3Cl^+ + I^-$	8.6×10^8	22	5.04
$NH_3Cl^+ + SO_3^{2-}$	2.9×10^9	24	5.1

[a] Conditions: 25.0 °C, μ = 0.50. [b] Anion nucleophilicity: Hine, J. *Physical Organic Chemistry*; McGraw-Hill: New York, 1962; p 161. [c] This work.

Comparison of Cl^+-Transfer Mechanisms. Recent studies[24] of the reactions between chloramine and sulfite show that the rates are general-acid assisted (eq 27) and occur by Cl^+ transfer to give

$$HA + NH_2Cl + SO_3^{2-} \rightarrow A^- + NH_3 + ClSO_3^- \quad (27)$$

chlorosulfate, which then hydrolyzes (eq 3). We know that sulfite reacts at chlorine rather than at nitrogen, because $SO_3NH_2^-$ is not detected as a reaction product.[24] Sulfamate is very slow to hydrolyze and would be seen if it formed.

Similar Cl^+-transfer mechanisms are proposed[25,26] for the reaction of HOCl with I^- and with Br^- as well as for the reaction in eq 10. Table VI compares values for the second-order rate constants for these reactions (a value of 28 M^{-1} is used for the protonation constant of NH_2Cl[27]) with the nucleophilicity[28] of Br^-, I^-, and SO_3^{2-}. The rate constants increase with the anion nucleophilicity (n) in agreement with the Swain and Scott relationship (eq 28).[29] This relationship was derived for reactions

$$\log (k/k_0) = sn \quad (28)$$

with nucleophilic attack at carbon, where typical values for s are 1.0 ± 0.5. Comparison of the HOCl results with Br^-, I^-, and SO_3^{2-} are given in Table VI, and Figure 7 plots log k values against n. The slope corresponds to an s value of 4.5 ± 0.3. Thus, reactions at chlorine are much more sensitive to the nucleophilic strength than reactions at carbon.

The rate constants for the reactions of SO_3^{2-} and I^- with NH_3Cl^+ are 4–6 times larger than with HOCl (Table VI). Ammonia is a suitable leaving group for the reaction of nucleophiles at the chlorine in NH_3Cl^+. As indicated, SO_3^{2-} must react at chlorine rather than at nitrogen. Iodide ion behaves similarly.

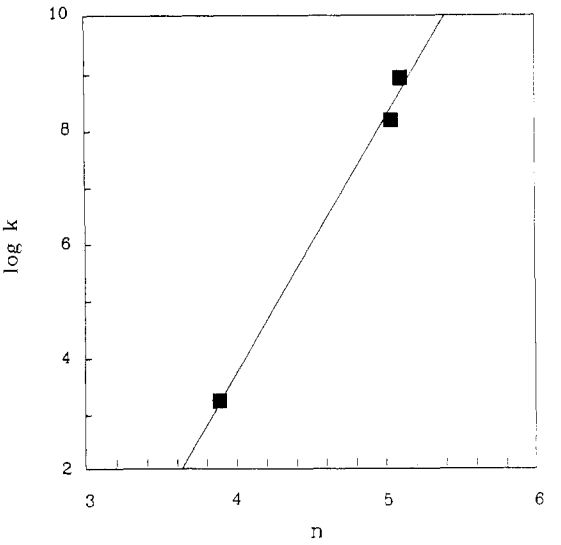

Figure 7. Swain–Scott plot of log k (for the reaction of HOCl with the nucleophiles Br^-, I^-, and SO_3^{2-}) versus the nucleophilicity of the anions. The slope is 4.5 ± 0.3.

The Br^- reaction with HOCl is 6.7×10^7 times faster than the Br^- reaction with H_2O_2.[26,30] This difference is consistent with a more favorable nucleophilic attack of Br^- on chlorine than on oxygen, because it is easier to expand the number of valence electrons around chlorine. Similarly, the reactions of I^- and of SO_3^{2-} with HOCl are factors of 2.3×10^8 and 4×10^9 faster than their reactions with H_2O_2. Hydroxide ion is a leaving group in all the H_2O_2 and the HOCl reactions.

The SO_3H^- ion is a much poorer nucleophile than SO_3^{2-}. This accounts for the preference for the HOCl, SO_3^{2-} reaction pair rather than the OCl^-, SO_3H^- pair. The proposed intermediate ($HOClSO_3^{2-}$) is a steady-state species rather than a preequilibrium species. Hence, it does matter where the proton is located originally. The OCl^-, SO_3H^- reaction pair does not have the required OH^- leaving group.

Proposed Oxygen Atom Transfer for OCl^- and SO_3^{2-}. At 25.0 °C the reaction of OCl^- with SO_3^{2-} is a factor of 3.3×10^4 smaller than the rate of the HOCl reaction with SO_3^{2-}. The transition state with OCl^- as a reactant does not have OH^- as a leaving group. If a Cl^+-transfer mechanism exists, then a proton would need to be transferred from water to give an $HOClSO_3^{2-}$ intermediate (eq 29), and this intermediate would react as previously

$$H_2O + OCl^- + SO_3^{2-} \underset{k_{-1'}}{\overset{k_{1'}}{\rightleftarrows}} (HOClSO_3^{2-}) + OH^- \quad (29)$$

$$(HOClSO_3^{2-}) \xrightarrow{k_5} OH^- + ClSO_3^- \quad (30)$$

postulated. Such a mechanism would also have to consider contributions from eq 9 and 18. We cannot assign reasonable values to $k_{-1'}$ that will permit the k_{obsd} values to be independent of the hydroxide ion concentration. Hence, this mechanism does not appear to be valid.

An alternate mechanism with SO_3^{2-} attack on oxygen and Cl^- displacement (an O atom transfer mechanism) appears to be required. The transition state in structure III is proposed. Although nucleophilic attack at oxygen is less favorable than at chlorine, the reaction is forced to find a pathway with a suitable leaving group (i.e. Cl^-). Sulfite attack on the oxygen of HOCl

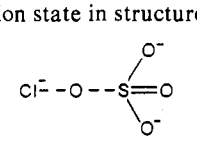

III

(25) Kumar, K.; Day, R. A.; Margerum, D. W. *Inorg. Chem.* **1986**, *25*, 4344–4350.
(26) Kumar, K.; Margerum, D. W. *Inorg. Chem.* **1987**, *26*, 2706–2711.
(27) Margerum, D. W.; Gray, E. T., Jr.; Huffman, R. P. In *Organometals and Organometalloids, Occurrence and Fate in the Environment*; Brinckman, F. E., Bellama, J. M., Eds.; ACS Symposium Series 82; American Chemical Society; Washington, DC, 1978; pp 278–291.
(28) Hine, J. *Physical Organic Chemistry*; McGraw-Hill: New York, 1962; p 161.
(29) Swain, C. G.; Scott, C. B. *J. Am. Chem. Soc.* **1953**, *75*, 141–147.
(30) Edwards, J. O. *Inorganic Reaction Mechanisms*; Benjamin: New York, 1964; pp 74–79.

is also possible and would have less electrostatic repulsion in the formation of the transition state, but the proton would also make it more difficult for Cl^- to leave. We propose that the factor of 3.3×10^4 difference in reactivity between OCl^- and HOCl is due to a change of mechanism from O atom transfer to Cl^+ transfer.

The previous ^{18}O-labeling experiments[2] with sulfite and hypochlorite were actually carried out in 0.2 M HCl where HOCl, Cl_2, SO_3H^-, and SO_2 were all present and the reaction mechanisms would very likely be completely different than is the case in NaOH solutions or in HCO_3^-/CO_3^{2-} buffer.

Conclusions

The rate of oxidation of SO_3^{2-} with HOCl is more than 4 orders of magnitude faster than the rate with OCl^-. A shift in mechanism from O atom transfer for OCl^- to Cl^+ transfer for HOCl is proposed to account for the huge increase in reactivity. Below pH 11 the rate of the oxidation can be limited by proton-transfer reactions. A reactive intermediate species, $HOClSO_3^{2-}$, is proposed, which reacts to form $ClSO_3^-$. The HOCl reactivity with $SO_3^{2-} > I^- > Br^-$ is highly dependent on the nucleophilicity of these anions.

Acknowledgment. This work was supported by National Science Foundation Grants CHE-8616666 and CHE-8720318.

Registry No. SO_3^{2-}, 14265-45-3; HOCl, 7790-92-3; OCl^-, 14380-61-1.

Contribution from the Department of Chemistry, The Florida State University, Tallahassee, Florida 32306-3006

Kinetics of Dissociation of Trivalent Actinide Chelates of TMDTA

Anthony C. Muscatello, Gregory R. Choppin,* and Willem D'Olieslager†

Received December 15, 1987

Measurements by a radiotracer technique show that the dissociation of TMDTA (trimethylenediamine-*N*,*N*-tetraacetic acid) chelates with Am, Cm, Bk, Cf, and Eu proceeds through an acid-catalyzed pathway. The rates of dissociation of $An(TMDTA)^-$ are 2 orders of magnitude faster than those of the corresponding EDTA chelates, presumably due to the greater lability of the nitrogen atom in the six-membered nitrogen–metal–nitrogen ring of TMDTA chelates. The rate of dissociation also decreased with decreasing metal ion radius. A proton-catalyzed mechanism similar to that for dissociation of EDTA complexes of lanthanide and actinide cations is consistent with the rate data.

Introduction

Studies of the kinetics of chelate complexation of the f elements are complicated by the ionic nature of the bonding in these complexes, as this results in relatively short-lived processes. The polydentate nature of the amino carboxylate complexes slows the rates of dissociation, allowing easier investigation. In these chelates, in which both carboxylate and amine donors are involved, questions arise about the rate-controlling processes in the bond formation and dissociation. Optical and NMR spectroscopies as well as metal exchange have been used to study the kinetics of lanthanide chelation.[1] The radioactive nature of the analogous trivalent actinide elements has restricted their study. However, the actinide systems that have been investigated show close similarity to the lanthanide complexes with the same ligands.

The exchange of trivalent actinides, An^{3+}, with $La(EDTA)^-$ complexes follows reversible first-order kinetics.[2-5] The rate equation for the exchange contained two terms, one dependent and one independent of the hydrogen ion concentration. The hydrogen ion dependent term was associated with proton-catalyzed dissociation of the lanthanide chelate. The free ligand then reacted with the actinide ion. The acid-independent term was interpreted as being due to a mechanism in which the actinide ion directly attacks and displaces the lanthanide in the complex.

Other studies of transplutonium element chelates include an investigation by El-Rawi[6] of the exchange kinetics of Am(III), Cm(III), and Cf(III) with lanthanum chelates that also reported acid-dependent and acid-independent terms in the rate equation. Makarova et al.[7] investigated Am(DCTA) and Cm(DCTA) dissociation rates using an electromigration method,[8] while Sullivan et al.[9] measured Am(DCTA) formation rates by stopped-flow spectrophotometry and dissociation rates by Cu(II) exchange. Both of these studies found acid-dependent and acid-independent pathways in the dissociative mechanism.

To better understand the factors involved in chelation kinetics, we have studied the dissociation of Eu(III), Am(III), Cm(III), Bk(III), and Cf(III) chelates of TMDTA (trimethylenediaminetetraacetic acid). TMDTA (also known as PDTA or 1,3-propanediaminetetraacetic acid) complexes would have one more carbon atom in the nitrogen–metal–nitrogen chelate ring than would EDTA complexes. Comparison of the stability constants of $Ln(EDTA)^-$ and $Ln(TMDTA)^-$ indicated that TMDTA complexes probably would have dissociation half-lives of a 1 min or less. Consequently, a solvent extraction system that allowed fast sampling was used. The development of this technique has been described previously.[10] We have also previously determined the stability constants of the chelates of Am, Cm, Bk, and Cf with TMDTA.[11]

Experimental Section

Reagents. Trioctylphosphine oxide, TOPO, from Eastman, was used without further purification. A 0.5 M solution was prepared by dissolving a weighed sample of TOPO in warm *n*-dodecane and diluting to volume. The solution was preequilibrated with an acetate buffer at a pH similar to that of the reaction solution (nonbuffered 0.5 M solutions of TOPO are supersaturated at room temperature).

TMDTA, trimethylenediaminetetraacetic acid, was synthesized by the method of Tanaka and Ogino[12] as revised by Ogino et al.[13] The pre-

† Present address: Department of Chemistry, The Catholic University of Leuven, Leuven, Belgium.

(1) Breen, P. J.; Horrocks, W. DeW., Jr.; Johnson, K. A. *Inorg. Chem.* **1986**, *25*, 1968.
(2) D'Olieslager, W.; Choppin, G. R. *J. Inorg. Nucl. Chem.* **1971**, *33*, 127.
(3) D'Olieslager, W.; Choppin, G. R.; Williams, K. R. *J. Inorg. Nucl. Chem.* **1970**, *32*, 3605.
(4) Choppin, G. R.; Williams, K. R. *J. Inorg. Nucl. Chem.* **1973**, *35*, 4255.
(5) Williams, K. R.; Choppin, G. R. *J. Inorg. Nucl. Chem.* **1974**, *36*, 1849.
(6) El-Rawi, H. Report KFK-1927; Karlsruhe Nuclear Research Center: Karlsruhe, FRG, 1974.
(7) Makarova, T. P.; Stepanov, A. V.; Gedeonov, A. D.; Maksimova, A. M. *Radiokhimiya* **1976**, *18*, 794; *Sov. Radiochem. (Engl. Transl.)* **1976**, *18*, 677.
(8) Stepanov, A. V. *Zh. Fiz. Khim.* **1973**, *47*, 1769; *Russ. J. Phys. Chem. (Engl. Transl.)* **1973**, *47*, 993.
(9) Sullivan, J. C.; Nash, K. L.; Choppin, G. R. *Inorg. Chem.*, **1978**, *17*, 3374.
(10) Choppin, G. R.; Muscatello, A. C.; D'Olieslager, W. In *The Rare Earths in Modern Science and Technology*; McCarthy, G. J., Rhyne, J. J., Eds.; Plenum Press: New York, 1978; p 135.
(11) Choppin, G. R.; Muscatello, A. C. *Inorg. Chim. Acta* **1985**, *109*, 67.
(12) Tanaka, N.; Ogino, H. *Bull. Chem. Soc. Jpn.* **1964**, *37*, 877.
(13) Ogino, H.; Takahashi, M.; Tanaka, N. *Bull. Chem. Soc. Jpn.* **1970**, *43*, 424.

0020-1669/89/1328-0993$01.50/0